Applied Energy 358 (2024) 122612

Contents lists available at ScienceDirect

Applied Energy

journal homepage: www.elsevier.com/locate/apenergy

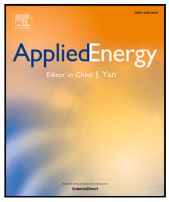

Reliability-based leading edge erosion maintenance strategy selection framework

Javier Contreras Lopez [a,*], Athanasios Kolios [b], Lin Wang [c], Manuel Chiachio [d], Nikolay Dimitrov [b]

[a] Naval Architecture, Ocean and Marine Engineering, University of Strathclyde, 16 Richmond St, Glasgow G1 1XQ, Scotland, UK
[b] Department of Wind and Energy Systems Structural Integrity and Loads Assessment, Technical University of Denmark, RisøCampus Frederiksborgvej 399, Roskilde 4000, Denmark
[c] Department of Mechanical, Materials and Manufacturing Engineering, University of Nottingham, Nottingham NG7 2RD, UK
[d] Department of Structural Mechanics and Hydraulic Engineering, Andalusian Research Institute in Data Science and Computational Intelligence (DaSCI), University of Granada, Granada, 18071, Spain

ARTICLE INFO

Keywords:
Leading edge erosion
Wind turbine blade O&M
Blade erosion degradation
Blade rain erosion
Wind turbine blade reliability

ABSTRACT

Leading edge erosion has become one of the most prevailing failure modes of wind turbines. Its effects can evolve from an aerodynamic modification of the properties of the blade to a potential structural failure of the leading edge. The first produces a reduction of energy production and the second can produce a catastrophic failure of the blade. Considering the uncertainties and constraints involved in the design of optimal operation and maintenance (O&M) strategies for offshore assets and the influence of site-specific parameters on the dynamics of this particular failure mode, the task becomes complex. In this study, a framework to evaluate the influence of different maintenance strategies considering uncertainties in weather, material behaviour and repair success is presented. Monte Carlo Simulation (MCS) is used alongside a computational framework for Leading Edge Erosion (LEE) degradation to evaluate the lifetime cost distribution and probability of failure of the chosen maintenance strategies. The use of the framework is demonstrated in a case study considering a 5-MW offshore wind turbine located in the north of Germany. The influence of the modification of the maintenance interval or time between repairs and the comparison with maintenance activities executed only during months with milder weather is analysed in terms of cost and reliability. A Pareto front plot considering the probability of failure and the median of the cost is used to jointly compare strategies considering both aspects to provide a tool for risk-informed maintenance selection. Finally, the potential benefits of condition-based maintenance and autonomous decision-making systems are discussed. The case of study shows the benefits of repairs during summer months and the importance of the relation risk/O&M cost for different maintenance strategies.

1. Introduction

The importance of renewable energy, and in particular, wind energy has increased steadily during the last decade. Recently, the interest for offshore wind has grown driven by the greater availability of space, the higher energy availability, and the lower social impact of the marine environment [1]. Some of the most important constraints to its growth are the high construction costs and the difficulties in the operation and maintenance (O&M) of the wind turbines, which can constitute a considerable percentage of their life cycle costs [2,3].

To address the problem of life cycle cost reduction, a proper understanding the wind turbine failure modes and their implications in cost and risk is a key aspect. In this line, the blades are one of the components carrying the highest cost and of which the maintenance and potential replacement have important influence in terms of planning, logistics, cost, and unavailability of the turbine [4]. While other mechanical components of the turbine have more complex condition monitoring systems such as the drivetrain or the bearings, the blades are usually inspected using time-based schedules either visually or with the aid of drones to identify potential damage. The difficulty of scheduling these campaigns in geographical zones with harsh weather conditions and the implications of damage or failure that require blade removal necessitate careful consideration.

Risk-based maintenance emerges as a potential solution to optimise maintenance planning. Nielsen and Sorensen [5] present an overview of the available risk-based planning methods for wind turbines in the literature. The same authors [6] also proposed a risk-based optimal

* Corresponding author.
E-mail address: javier.contreras-lopez@strath.ac.uk (J.C. Lopez).

https://doi.org/10.1016/j.apenergy.2023.122612
Received 15 September 2023; Received in revised form 27 November 2023; Accepted 30 December 2023
Available online 16 January 2024

Table 1
Leading edge damage classification by severity [11].

Damage type	Severity	Action recommended by [12]
LE discolouration, paint or bugs	1	No need for immediate action Continue normal turbine operation
Coat/paint damage, surface: Missing less than 10 cm^2	2	Repair only if other damages are to be repaired Continue normal turbine operation
Coat/paint damage, surface. Missing more than 10 cm^2 Damaged leading edge protection Damaged leading edge tape LE erosion, down to laminate	3	Repair within 6 months Continue normal turbine operation
LE erosion, down to laminate and first layer laminate	4	Repair within 3 months and monitor damage Continue normal turbine operation
LE erosion, through laminate/Open LE	5	Repair immediately Stop turbine operation

planning method. The proposed approach considers the optimisation from the design stage, considering some candidate designs, to the final decommissioning of the turbine and bayesian updating to incorporate any available information that can improve the decision-making such as Structural Health Monitoring (SHM), inspection data or data from other turbines. Morato et al. [7] propose a combination of dynamic Bayesian networks with Partially Observable Markov Decision Processes (POMDPs) in a joint framework for optimal inspection and maintenance planning in problems dominated by structural reliability. This proposed framework is compared with classic heuristics-based policies showing a better performance. Nielsen et al. [8] estimate the value of information of a vibration-based SHM system through bayesian networks and MCS using the computational framework proposed in [9]. Dimitrov [10] presented a risk-assessment for wind turbine blade damages observed during visual inspection demonstrated on LEE and trailing edge cracks.

Depending on the severity of LEE damage sustained, the repair process can encompass a wide range of techniques, from the application of coatings, tapes, or shields for minor damage, to filling and sealing techniques or resin injection for non-structural matrix cracks, small surface cracks, or delamination, to the use of composite laminate patching for structural damage. A classification of damage according to its severity is shown in Table 1. The time required for repair can vary greatly, and in certain cases, the disassembly of the blade may be needed if the damage is critical. Fig. 1 shows an example of leading edge blade repair. The challenges associated with performing the repair without disassembly, coupled with the difficulties of accessibility, workforce safety, and weather-related constraints, present significant obstacles in the successful completion of wind turbine blade repair missions. Therefore, it is essential to carefully plan its maintenance to overcome these challenges and improve the efficiency and safety of wind turbine blades. There are guidelines in the literature, such as the provided by Bladena [11], that contain recommendations for operation and maintenance actions related to LEE. It is suggested that repairs should be done within 6 months if the erosion reaches the laminate and within 3 months if it reaches the second layer of the laminate to prevent compromising the structural integrity of the whole blade.

The problem of LEE on wind turbine blades is met with a diverse array of solutions. These include the use of protection tapes, protective coatings, and epoxy or polyurethane fillers. Protective coatings are relatively quick to install and may offer reliable protection but can also alter the original aerodynamics of the blade, potentially impacting Annual Energy Production (AEP). Epoxy and polyurethane fillers require a more labour-intensive application process and may be impacted by weather conditions such as temperature and relative humidity. On the other hand, tapes or sheets, which are easy to install and have fewer weather-related restrictions, may be a viable option. However, the lifetime of each solution and its cost-benefit and suitability for a specific site are not yet fully understood [13], as research on this topic is still ongoing.

The potential criticality of blade erosion-related failures [15], the difficulties to access offshore wind turbines for inspection and maintenance due to the harsh weather conditions of some regions and the uncertainty in the evolution of this failure mode increase the importance of adequate maintenance scheduling given that the miss of a maintenance opportunity window can lead to a late maintenance and suboptimal operation of the asset or even a catastrophic failure of the blade. In response to this, the present manuscript aims to provide a framework for the maintenance planning of leading edge erosion of offshore wind turbine blades based on reliability and considering the uncertainty in weather, damage evolution and the success on the planning and execution of the maintenance missions. This framework can be of great use for baseline maintenance planning at wind farm level when the need to consider different failure modes and conditions for a number of failure modes and turbines can increase the complexity of the problem making it difficult to be scheduled efficiently.

Designing O&M policies for wind energy assets is a non-trivial task requiring a multi-level and site-specific approach. The first step is being able to obtain a good representation of the dynamics of high priority failure modes at low-level (component/subcomponent level), which is the foundation for an accurate description of the system. It is important that the low-level modelling is able to capture the most important sources of uncertainties (material and weather among others) related to each of the failure modes considered. For some offshore locations, the constraints and particularities of a site can widely modify the evolution of particular failure modes and the characteristics for optimal policies. The next step would be the joint analysis of the relevant failure modes of different components of the system. For this step to be performed, a description of the evolution of the failure modes considered by efficient surrogate models may be required for a computationally affordable simulation of different maintenance strategies. Finally, a reliability analysis of the system is to be performed in order to make risk-informed O&M strategy decisions for the asset that align with the tolerance to risk of the organisation managing the asset.

In this study, a framework for risk-based maintenance strategy selection for leading edge blade erosion is proposed. This method provides an approach for O&M operators to design baseline calendar-based site-specific maintenance strategies at wind farm level using rain test erosion experiment data. One of the novelties of this work is the consideration of uncertainty in weather and coating durability. A reliability function for this failure mode is proposed to obtain the probability of failure of the proposed maintenance policies. A Pareto front plot is then drawn considering risk and cost metrics such as the accumulated Probability of Failure (PoF) at the end of the lifetime and median of O&M lifetime costs, respectively, to aid in the design of the policy.

The manuscript is structured as follows. Section 2 provides a description of the methodology used, the definition of the reliability function and the stochastic variables considered for the reliability analysis. Section 3 presents all the assumptions considered in the

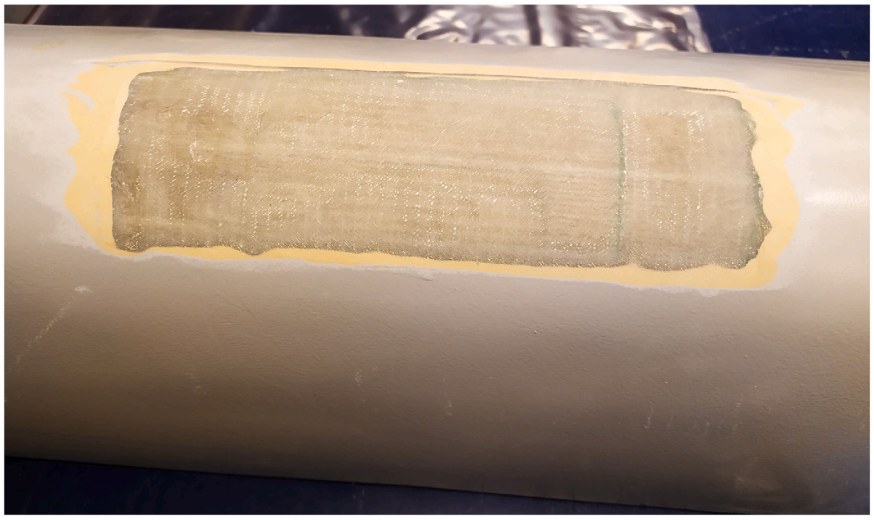

Fig. 1. Repaired leading edge of the wind turbine blade (demonstration of composite repair by Danish Blade Service Aps). *Source:* [14].

O&M simulations. A case study demonstrating the use of the proposed framework and considering a 5-MW turbine is presented in Section 4. Finally, the conclusions of this study are presented in Section 5 and the potential of condition-based maintenance is also discussed.

2. Methodology

The proposed framework for risk-based maintenance strategy selection for leading edge blade erosion is presented here. The first step in the framework is the definition of the stochastic variables to consider in the study. In this case, model parameters governing the dynamics of the evolution of LEE and site-specific environmental parameters (namely, wind speed, u, and rain intensity, I) are considered as stochastic variables to analyse the reliability of the blade affected by leading edge erosion. Second, the definition of the LEE damage threshold for the reliability function defining the failure of the blade. Then, candidate O&M policies are simulated through MCS to obtain their lifetime cost distribution and Probability of Failure (PoF). Two type of policies are considered, namely policies based strictly on the calendar, labelled as *SM*, and others based on a maintenance interval or time between repairs, labelled as *TBR*. In this work, maintenance interval is defined as the time threshold over which a maintenance action is scheduled after a successful repair. For *SM* policies, maintenance is attempted once the planned maintenance month is reached until success. In the case of *TBR* policies, a time interval from the last performed maintenance is defined. Once this interval is reached, maintenance actions attempted until weather constraints allow their completion. With the results of the simulations using the candidate policies, a Pareto front plot can be drawn in order to identify the policy that meets the requirements of a predefined maintenance strategy, providing a way to make risk-informed decisions. The suggested metrics for the Pareto plot are the median of the cost and the accumulated PoF at the end of life following a specific policy. Fig. 2 provides a scheme to better clarify the main calculation steps of the proposed methodology.

This study is focused on the leading edge erosion failure mode and will be the only one considered for the reliability-based maintenance optimisation. As commented above, this failure mode develops over time and requires timely maintenance to avoid the structural failure of the blade. For the reliability analysis, a performance function $g(X)$ is needed. In the case of leading edge erosion, the following performance function can be defined:

$$g(X,t) = p - d(X,t) \tag{1}$$

where p is the selected damage threshold, X the set of stochastic variables affecting erosion damage progression and $d(X,t)$ is the accumulated erosion damage at time t. Damage progression can be calculated as:

$$d(X,t) = \sum_{i=0}^{i=t} \frac{h_i}{H} \tag{2}$$

where h_i is the accumulated rain impingement h during time step i and H the accumulated rain impingement to erosion failure of the coating resulting from Whirling Arm Rain Erosion Test Rig (WARER) or Rain Erosion Tester (RET) tests, which is considered as the equivalent of damage severity 5 from Table 1. The accumulated rain impingement to erosion failure, H, can be obtained as:

$$H = C_1 \cdot v(r)^{-C_2} \tag{3}$$

being C_1, C_2 model parameters describing the durability of the system and calibrated using experimental WARER test data for a specific protection system.

The computation framework used in this study is taken from [16] and reproduced here under a concise and unifying notation, for clarity. A schematic of this framework is shown in Fig. 3. To address the impact of uncertain site-specific weather conditions, the proposed methodology commences with the generation of stochastic wind and rain time series. These can be derived from either observed meteorological data or ERA5 reanalysis data for the precise location of the wind turbine [17]. In the absence of data, the aerodynamic effects of LEE can be estimated through 2D or 3D Computational Fluid Dynamics (CFD) simulations or experimental testing, such as wind tunnel experiments of eroded airfoils. Given the significant computational expense of each simulation, and the number of simulations necessary to capture the various stages of blade degradation, the 2D modelling approach is preferred in this study. The maximum expected aerodynamic losses for a severe degradation state can be estimated using the 2D CFD method on the different airfoils conforming the last third of the blade by adjusting the sand grain roughness height, k_s, to a value of $k_s/c = 0.0076$, where c is the chord of the airfoil, as proposed in [18]. Intermediate degradation states can be linearly interpolated considering the damage state of the section of interest. Moreover, the use of the Blade Element Momentum (BEM) theory enables the integration of numerically or experimentally obtained polar curves in a more practical and efficient manner, as shown in [19], given that different combinations of damage states along the blade can be considered in a more efficient way than a 3D CFD simulation. Once the aerodynamic efficiency of eroded airfoils has been

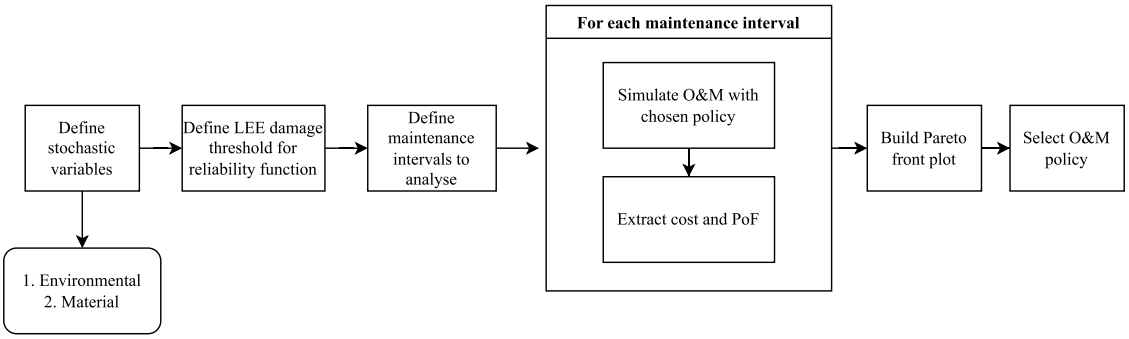

Fig. 2. LEE risk-based O&M policy selection.

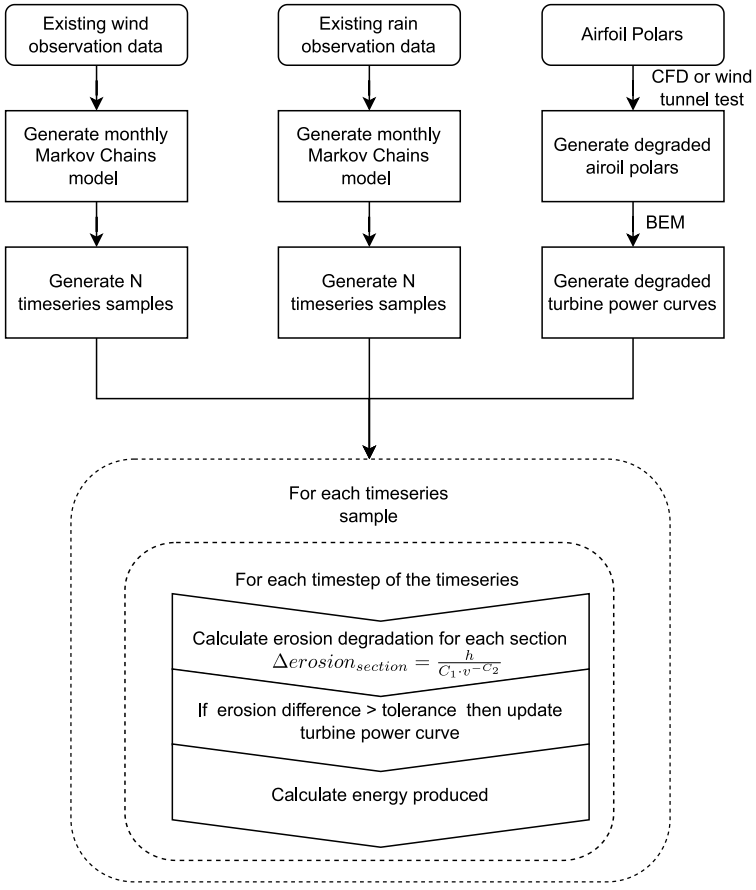

Fig. 3. LEE calculation framework.
Source: [16].

estimated, the power production of the wind turbine across different degrees of blade erosion can be computed. A number of calculation points are defined in the last third of the blade, which is the area more prone to LEE. For the calculation points defined, d is calculated at every time step. Lift values of the airfoils are linearly interpolated for discrete degradation states. In the current study, damage was discretised every 10% increase. The synthetic weather data and the estimated aerodynamic performance of airfoils are subsequently merged to estimate LEE degradation and energy production at each time step, using the appropriate power curve that represents the degraded state of the blade under the BEM theory. The reader is referred to [16] for a detailed view of the used approach and validation.

2.1. Limit states/design criteria

Linear degradation has been assumed for the LEE failure mode. In this study, damage, d, is defined in the interval [0,1]. The physical meaning attributed to different physical degradation states of the blade is shown in Fig. 4. The intervals between different damage severity categories can be tuned using a thorough WARER test campaign or based on experience of operation data of turbine blades using similar coatings. This categorisation is used to assign meaningful repair costs to the different degradation states. The evaluation of the performance function requires a careful selection of the abovementioned damage threshold, p. In this case, a value of 0.8 was chosen for the damage

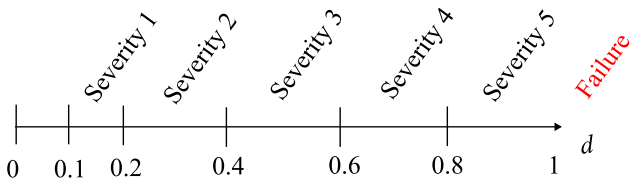

Fig. 4. Damage, d, assigned to different damage severity categories.

threshold representing the beginning of damage to the laminate (transition from severity 4 to severity 5), which requires a careful repair treatment to avoid the damage evolution that could develop into a catastrophic failure of the blade. Damage above this level could lead to difficult repairs of the blade requiring its disassembly or catastrophic failures leading to a large downtime. The failure of the blade is then considered when $g(X,t) \leq 0$. For the computation of the PoF this study assumes the failure of the blade from a specific time step t even if the blade is restored to a working condition $g(X) > 0$. The PoF is obtained by MCS and computed as:

$$PoF(t) = \frac{f(t)}{n} \tag{4}$$

where $f(t)$ is the number of failures at a given time step and n the number of simulations.

2.2. Selection of stochastic variables

In this study, both parameters C_1 and C_2 describing the durability of the coatings and site-specific environmental parameters wind speed, u, and rain intensity, I are considered as stochastic variables to analyse the reliability of the blade affected by leading edge erosion.

2.2.1. Model parameters C_1 and C_2

This framework allows the consideration of the uncertainty in the results of experiments on the model parameters of the protection system. This approach overcomes the limitations of relying solely on a deterministic value for the entire population, which may not accurately reflect the behaviour of each individual. By conducting experiments with varying drop sizes and rotation speeds, the uncertainty in the results can be taken into account for the maintenance of the blades, thereby preventing an unnecessary increase in maintenance costs and avoiding catastrophic failures. A proper definition of these parameters allows us to include test data using different testing conditions. To this end, confidence intervals can be defined with the number of tests performed on the coating and the fitting parameters C_1 and C_2. Fig. 5 shows this approach for a specific coating defined in [20].

2.2.2. Climatic variables

Acquiring high-granular and high-quality weather time-series data for a specific wind farm location over extended periods can be challenging and costly. To account for site-specific weather conditions, uncertainty in wind speed u and rain intensity I has been considered in this framework. Depending on the availability of data for the location, different approaches can be applied.

The solution proposed to generate synthetic wind speed datasets that mimic the weather patterns at the site of interest considers the use of Markov chain models [21]. The generated datasets must cover a period of 20 to 25 years, which encompasses the expected service life of the turbine. This study utilises 10-minute average data for wind speed and rain intensity. The wind data is modelled using a Markov probability transition matrix with 0.5 m/s bins, calibrated using FINO1 10-minute average wind speed observation data [22]. A finer discretisation would produce a distribution closer to the observations at the expense of a greater amount of data for the calibration of the transition probability matrices. The process can be summarised in the following steps:

1. Calibration of the generative model:
   (a) Binning the observations of wind speeds using the desired bin width monthly and annually.
   (b) Computing the transition probabilities by counting the number of wind speed transitions from each of the bins to the rest of the bins.
2. Generation of synthetic time series:
   (a) Initialise wind value from histogram of observations. The wind speed value is drawn from a uniform PDF within the limits of the drawn bin.
   (b) Drawing the next wind value bin using the transition probabilities of the current bin.
   (c) Next wind value is drawn from a uniform PDF within the limits of the current bin.
3. Postprocessing: The first year of the synthetic series can be removed to reduce the bias.

To account for the seasonal variation of average wind speeds, separate probability transition matrices for each month, in addition to a general annual wind transition probability matrix, are considered to ensure that wind speeds fall within observed ranges.

In the case of rain intensity an alternative approach is required given that the available data range was limited. The approach considered in this study is described here:

1. Using ERA5 reanalysis data, fit monthly probability density functions for rain intensity. In this case, Weibull PDFs were used.
2. From the reanalysis data, calibrate a simple Markov chain model considering 2 states (Raining and not raining) and the transition probabilities from each of them to the other states.
3. For data generation, every time step a rain state will be drawn. When the state is *raining*, the rain intensity will be drawn from the site-calibrated Weibull PDFs.

ERA5 reanalysis data can be obtained to fit monthly Weibull probability density functions of 10-min average rain intensity data. In addition, Markov probability transition matrices for rain/no rain probability can be generated. When combining these techniques, rain intensities are drawn for the monthly fitted density functions when the rain state is drawn from the Markov chains. While this approach may result in abrupt variations in rain intensities, it will not significantly affect the results of the study since the relative variation of rain intensity is assumed not to affect the degradation rate of the blade. In this study, wind and rain have been modelled as statistically independent variables.

3. O&M model assumptions

For the O&M simulations, the following assumptions were considered:

- Only the O&M costs of the blade due to LEE are considered as defined in Table 2 and obtained from [8,23].
- Operation of the turbine is assumed to start at the beginning of January.
- Imperfect repairs. After each repair, the true damage state of every calculation point, d, is set to a value drawn from a normal distribution $d \sim \mathcal{N}(\mu, \sigma^2)$ with $\mu = 0.05$ an $\sigma = 0.001$ and truncated at the interval $[0, 1]$ to avoid values out of the defined interval for d.
- Imperfect inspection is considered. Inspected damage, D, follows a Gaussian distribution with $\mu = d$ and $\sigma = 0.1$, truncated at the interval $[0, 1]$ to avoid values out of the defined interval for D.

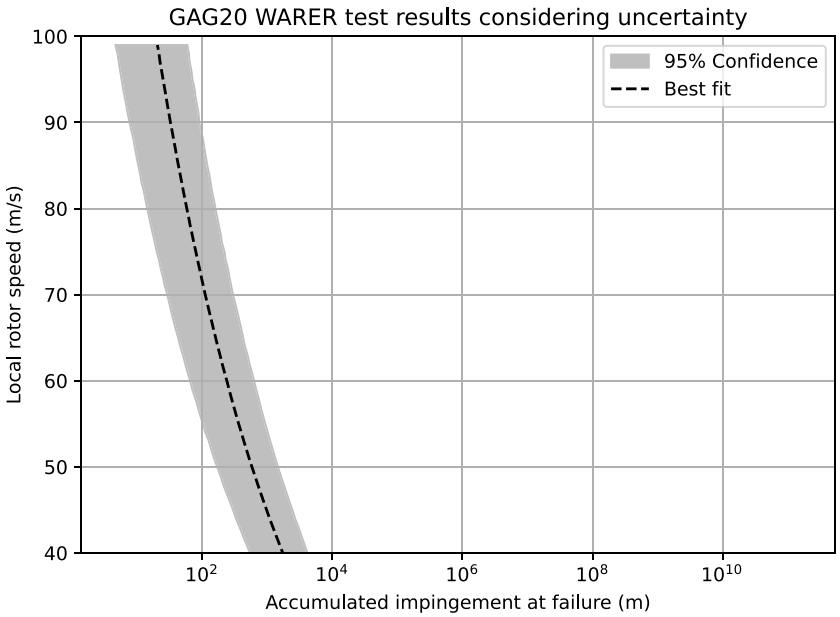

Fig. 5. Accumulated impingement at failure for GAG20 coating.

- If any of the calculation points of the blade reaches $d = 1$, the turbine will be preventively stopped until its repair/replacement. This study assumes that when the blade reaches that degradation step, other systems such as SCADA will produce alarms and the turbine will be preventively stopped.
- Energy cost of 50 £/MWh is considered, which is in line with the Contracts for Difference (CfD) strike price signed for CfD4 in 2022 in the UK.
- Probabilistic definition of repair success discretised by month and trying to mimic the real O&M scheduling. The associated cost of a repair is a function of the damage and the month at which the repair is attempted. This is defined in Section 3.1.
- For calendar-based scheduled maintenance strategies (labelled as *SM*), repairs are attempted until success when the scheduled date arrives. In these policies, maintenance is planned for a specific calendar month (i.e. June) and is attempted until success irrespective of what the state of the blade is.
- For time between repair maintenance strategies, labelled as *TBR*, a time between successful repairs threshold is defined. Once the threshold is surpassed, repairs are attempted until weather constraints allow their completion.
- Energy production losses due to the reduced aerodynamic performance of the blade caused by erosion are considered following the calculation framework from [16].
- Energy production losses due to downtime and preventive stops are also considered.

3.1. Repair modelling

Repair costs have been discretised according to the erosion damage level of the blade. The costs considered are shown in Table 2. Repair costs are made of 3 factors:

$$C_m = m_b + m_a + m_e \tag{5}$$

Being m_b the booking cost for the logistics and staff required for the inspection/repair, m_a the access cost to the turbine and m_e the execution cost of the maintenance activity. The costs of maintenance activities depending on the severity of the damage are shown in Table 2.

In this study, the probabilities of repair success have been modelled in three steps. First, the probability of a given month having wind speed values below the constraints shown in Table 3, P_1. These constraints have been adopted from [24]. Second, the probability of the forecast weather to comply with a required weather window, P_2. Finally, the probability of the real weather to comply with a required weather window, P_3. These probabilities have been obtained through MCS for each month and damage severity. Weather time series have been built using the framework shown in [16]. Synthetic significant wave height, H_s, data has been created through a Artificial Neural Network (ANN) trained using FINO1 data. The chosen fully connected ANN architecture is composed of an input layer, a hidden layer of 4 neurons using the sigmoid activation function and the output layer. The ANN The parameters used for the ANN are described here:

Table 2
Repair costs per damage severity - 3 blades. Data obtained from [8] and [23].

Damage severity	m_b (£)	m_a (£)	m_e (£)
0 (Inspection)	1600	1000	3200
1	2000	1000	4000
2	2000	1000	4000
3	3000	1000	6000
4	5000	1000	36,000
5	0	250,000	3,500,000
6	0	250,000	5,000,000

- $H_{s_{i-1}}$: Average significant wave height of the previous time step.
- $H_{s_{i-2}}$: Average significant wave height of 2 time steps ago.
- W_i: Current average wind speed.
- W_{i-1}: Average wind speed of previous time step.
- W_{i-2}: Average wind speed of 2 time steps ago.
- M_i: Month of time step i.

In order to verify the quality of the H_s generative model, it has been tested in an unseen dataset of 22,000 samples. The distribution of H_s for the synthetic data and observations and the calibration plot are shown in Fig. 6 showing a good agreement and therefore a good potential for the generation of synthetic H_s time series for the location of the project.

A sample of the ANN outcome when compared with FINO1 data is shown in Fig. 7. The weather restrictions parameters to comply for a successful weather window are significant wave height and 10-min average wind speed at hub height. It is assumed that for the case of P_3, the real weather deviates from the forecast with a growing

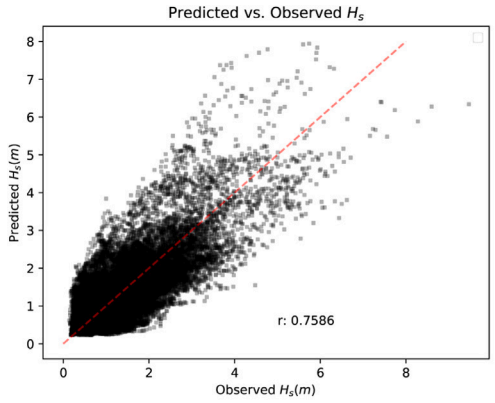

(a) Wind speed distribution - Observed vs Synthetic data.

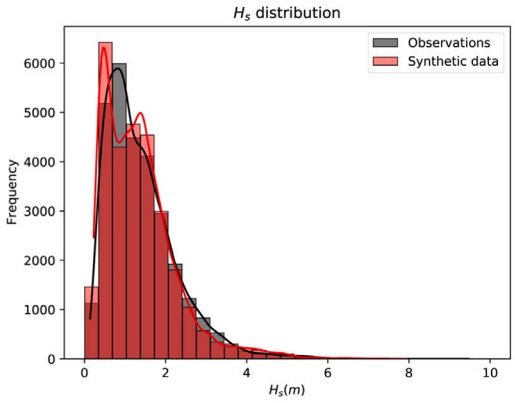

(b) Distribution of H_s - Observed vs Synthetic data.

Fig. 6. Weather data used in the case study.

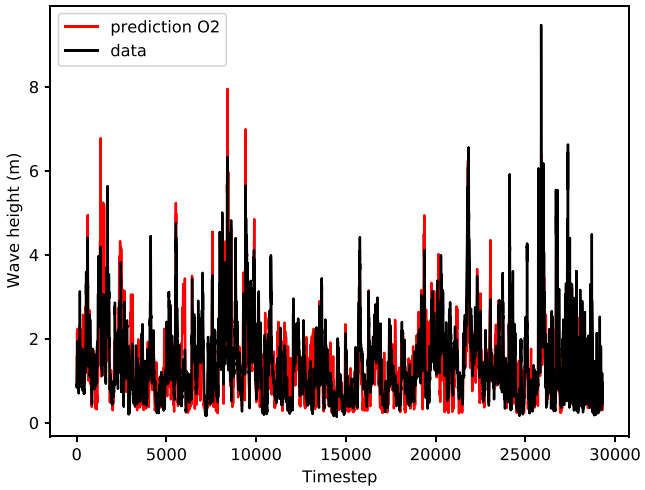

Fig. 7. Sample H_s prediction.

uncertainty. This has been modelled as a Gaussian distribution centred on the forecast value with a standard deviation that grows a 4% daily.

The modelling of the repair success and the associated cost of each of the repair outcomes is depicted in Fig. 8.

Repair success probability matrices P_1, P_2 and P_3 for the study case are shown in Appendix A.

3.2. Repair constraints

The repair constraints considered for the study are based on the weather restrictions assumed by [24] and summarised in Table 3.

3.3. Cost model

The O&M cost for the simulations is calculated as follows:

$$C = C_l + C_m + C_d \tag{6}$$

where C_l is the cost of the energy lost due to the degradation caused by the ageing of the turbine and the aerodynamic performance of LEE; C_m is the maintenance costs including the costs of booking, logistics and performance of the repair for all the maintenance activities performed on the blades; and C_d are the losses produced by the downtime of the turbine due to its preventive stop to avoid catastrophic failures or the repair of the blades.

4. Case study

To demonstrate the utility of this framework, a case study using an NREL 5-MW fixed-bottom wind turbine [25] located in the vicinity of FINO1 offshore measurement platform, sited 45 km north of the coast of the island of Borkum, Germany. Wind speed data was obtained from the FINO1 database and rain data from ERA5 reanalysis. Wind and rain synthetic data is shown in Fig. 9.

The maximum effects of erosion considered for the calculations derived from 2D CFD simulations of pristine and eroded airfoils are shown in Fig. 10. The degraded power curve represents an expected AEP loss for the site between 1.46% to 1.78% [16] with a LEE degradation of the last third of the blade. The coating of the blade considered for this study is a generic blade coating system supplied by Olsen Wings A/S from [20]. For each of the runs, C_1 and C_2 are drawn from normal distributions with mean and standard deviation as shown here: $C_1 \sim \mathcal{N}(1.45 \cdot 10^{11}, 0.05 \cdot 1.45 \cdot 10^{11})$ $C_2 \sim \mathcal{N}(4.98, 0.02 \cdot 4.98)$. These distributions for the model parameters are derived from the WARER test results using G20 needles, 3.5 mm droplet size, found in [20], and represent damage evolution rates in the range of others found in the literature [26,27]. The uncertainty in the behaviour for different droplet sizes in the WARER test was not considered in this case study.

The maintenance strategies analysed for this case are divided in two types, calendar-based scheduled in the months of summer and time-between repairs. The analysed strategies are summarised in Table 4.

Every of the maintenance strategies was run for 50,000 simulations for the 25 years of the lifetime of the turbine. In the case of *TBR* maintenance strategies, the trigger for maintenance is the time since last repair. Once it is reached, the maintenance is attempted until being successful. For *SM* maintenance strategies, repairs are attempted once the scheduled calendar month arrives until the maintenance is executed successfully.

4.1. Reliability analysis

The reliability of the blade using the different maintenance strategies has been studied using Eq. (1). The reliability and PoF over the life time of the turbine are shown in Fig. 11. The PoF was calculated after running 50,000 independent simulations. The average reliability at time t_k, $\bar{g}(t_k)$, can be defined as follows:

$$\bar{g}(t_k) = \frac{1}{n}\sum_{i=1}^{n} g_i(X, t_k) \tag{7}$$

Similarly, the average reliability over the lifetime of the turbine, $\bar{G}$ can be defined as:

$$\bar{G} = \frac{1}{n \cdot T}\sum_{i=1}^{n}\sum_{t_k=T_0}^{T} g_i(x, t_k) \tag{8}$$

Table 3
Weather repair constraints.

Damage category	Logistic requirements	Duration (h)	Max. significant wave height (m)	Max 10-min wind speed (m/s)
1: LE discolouration, paint or bugs	CTV, rope access	6	1.5	11
2: Coat/paint damage, surface: Missing less than 10 cm^2	CTV, rope access	15	1.5	11
3: Coat/paint damage, surface: Missing more than 10 cm^2 Damaged leading edge protection Damaged leading edge tape LE erosion, down to laminate	CTV, rope access	18	1.5	11
4: LE erosion, down to laminate and first layer laminate	CTV, crawler platform	40	1.5	12
5: LE erosion, through laminate/Open LE	HLV, blade disassembly	72	1.8	10
6: LE erosion, blade failure	HLV, blade disassembly	72	1.8	10

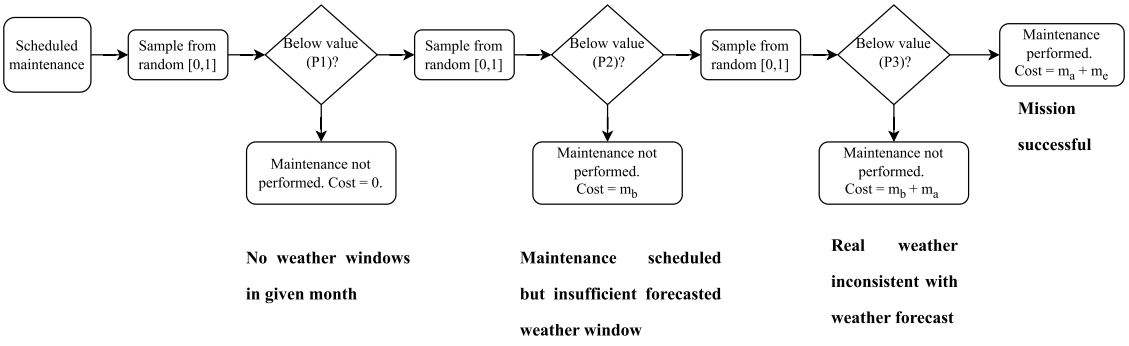

Fig. 8. Repair modelling.

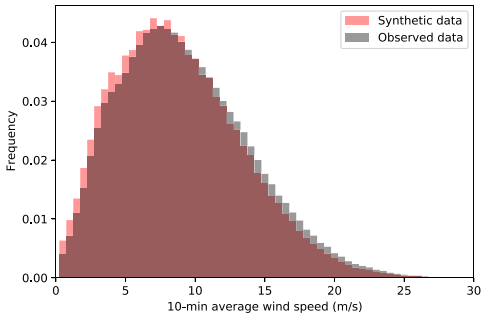

(a) Wind speed distribution - Observed vs Synthetic data.

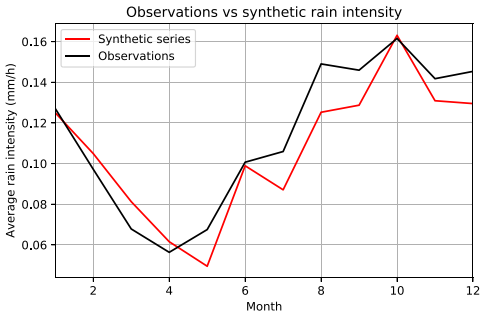

(b) Average rain intensity - Observed vs Synthetic data.

Fig. 9. Weather data used in the case study.

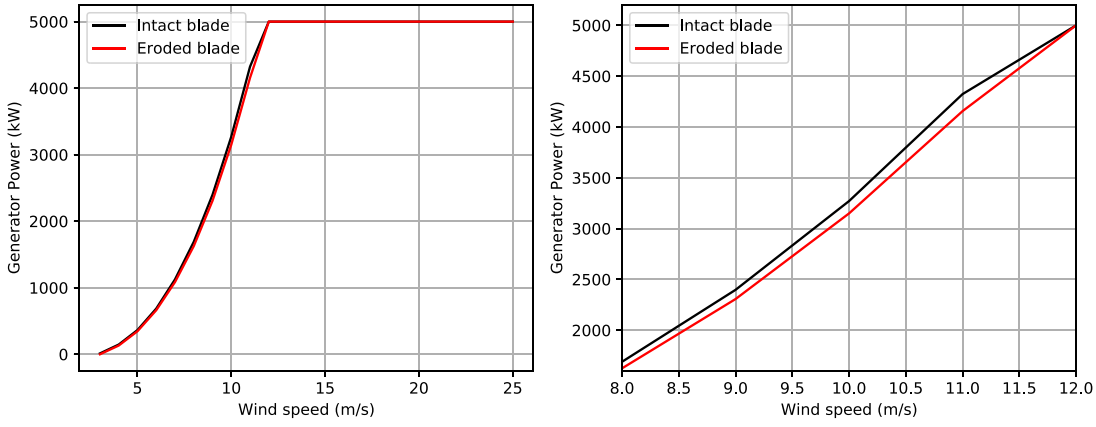

Fig. 10. Wind turbine power curves for pristine and eroded states.

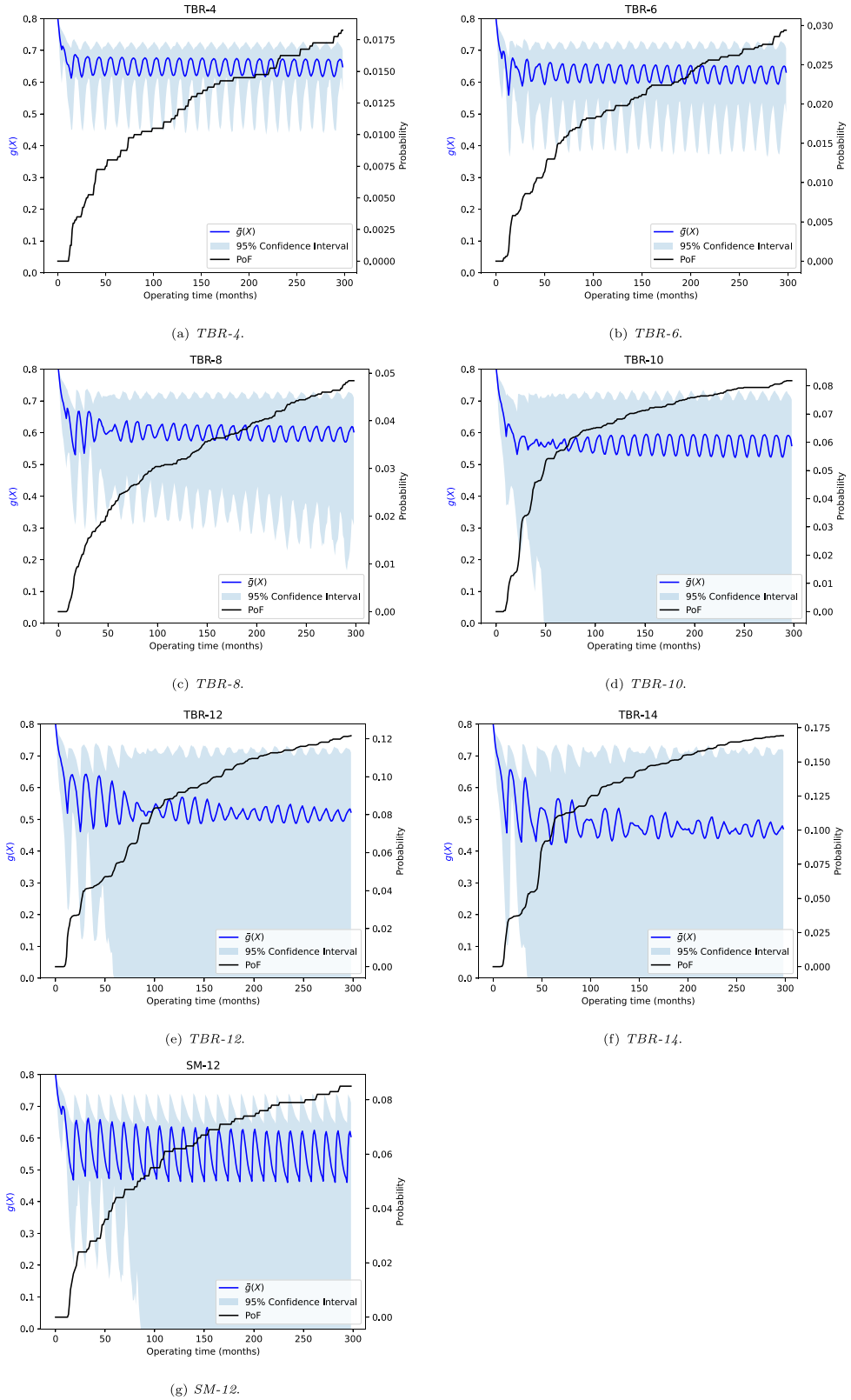

(a) *TBR-4.* (b) *TBR-6.* (c) *TBR-8.* (d) *TBR-10.* (e) *TBR-12.* (f) *TBR-14.* (g) *SM-12.*

Fig. 11. Reliability analysis. The left axis represents the reliability $g(x)$ of the LEP system, the right axis represents the cumulative probability of failure.

being T_0 and T the initial and final month of operation of the turbine, respectively.

In terms of reliability, it can be observed a first non-stationary phase in which failures having a lower time to failure than time to first maintenance appear and increase the accumulated PoF. After this phase, the rate of increase of PoF over time decreases until it is reduced to a small value. The accumulated PoF values at the end of the service life are summarised in Table 5. As expected, PoF increases with the increase in time between repairs. The lower repair success probability during winter months is noted by the difference in the PoF and $\bar{G}$ of

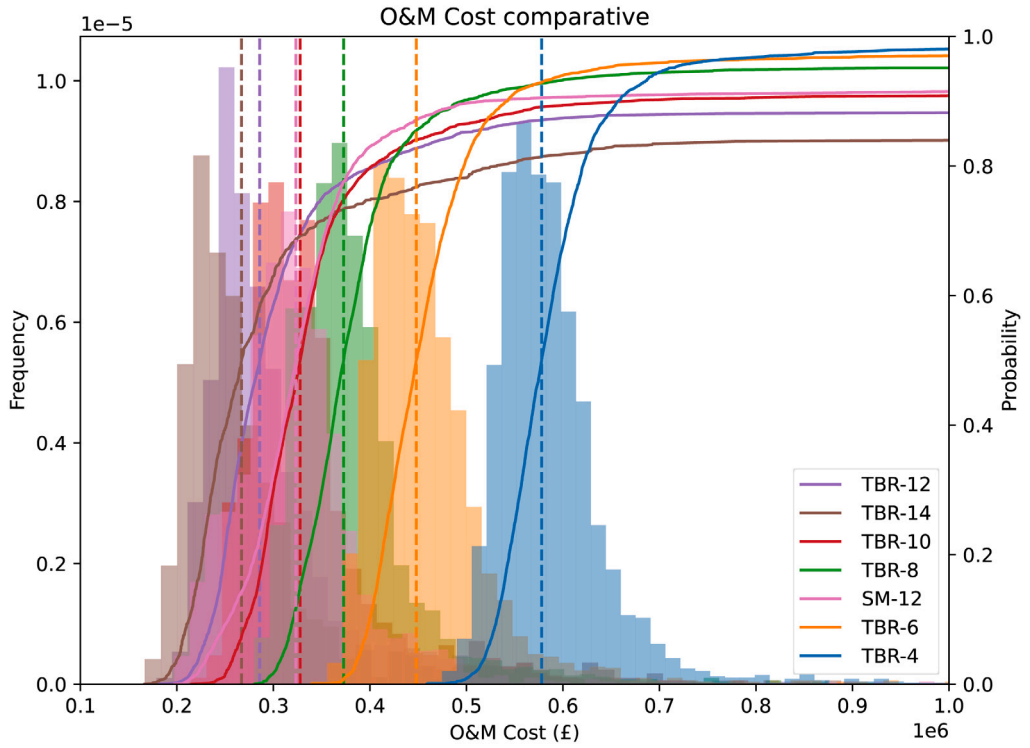

Fig. 12. Total O&M cost distribution for analysed maintenance strategies. The left axis represents the frequency and the right axis the cumulative probability of occurrence. The dashed line represents the median of the O&M strategy. The cumulative probability of occurrence tends to 1, but the plot was truncated at 1M for a better visualisation of the distribution of the costs.

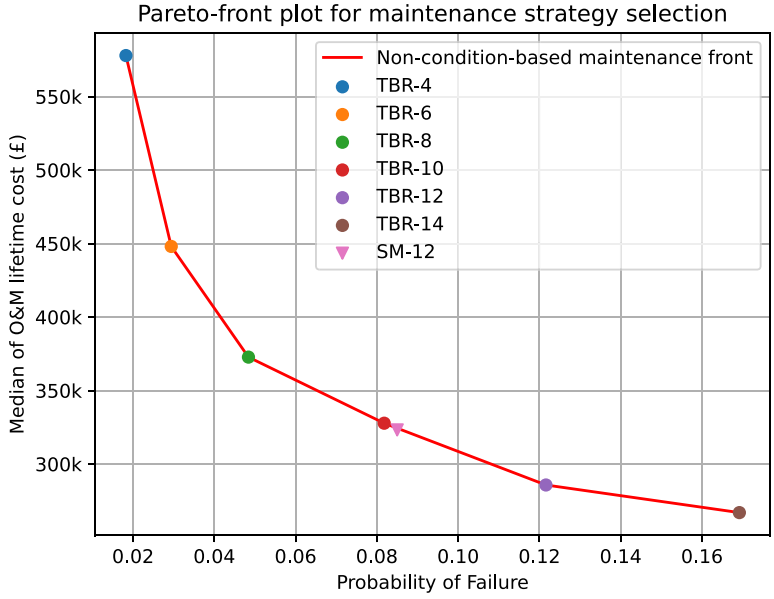

Fig. 13. Pareto front plot - O&M decision-making.

maintenance strategies *SM-12* and *TBR-12* for which PoFs are 0.0850 and 0.1216 and average $\bar{G}$ of 0.5577 and 0.5360, respectively.

4.2. Cost analysis

O&M costs for the maintenance strategies analysed have been obtained considering the ageing and erosion losses, downtime losses and maintenance costs. The total cost distributions are shown in Fig. 12. This figure presents the effects of an increased number of maintenance activities, with an increase on the median of the cost and a reduction of its variance with the decrease of time between repairs. There is a trade-off between the probability of failure and the median of the O&M cost.

4.3. Pareto front analysis

A Pareto front analysis of the results obtained through the simulations is presented in Fig. 13. In this case, the median and the PoF were chosen as representative values for the decision-making of this failure mode, although these metrics can be chosen as per the organisation's

Table 4
Maintenance strategies analysed.

Label	Description
SM-12	Repairs every June (annually)
TBR-4	Repairs every 4 months
TBR-6	Repairs every 6 months
TBR-8	Repairs every 8 months
TBR-10	Repairs every 10 months
TBR-12	Repairs every 12 months
TBR-14	Repairs every 14 months

Table 5
End of Life (EoL) reliability summary.

Label	PoF at EoL	$\bar{G}$
TBR-4	0.0183	0.6522
TBR-6	0.0294	0.6307
TBR-8	0.0484	0.6054
TBR-10	0.0818	0.5695
TBR-12	0.1216	0.5360
TBR-14	0.1692	0.4936
SM-12	0.0850	0.5577

requirements. This step is critical for a risk-informed decision-making. In this particular case, it can be noted that there is a trade-off between the median of the O&M cost and the PoF of the LEE. By analysing the different strategies, it can be observed that the relation of the increase in PoF and the decrease in median cost is non-constant. Once this information is ready, the most appropriate maintenance strategy according to the policy of the organisation operating the asset can be selected.

5. Conclusions and further remarks

This paper presents a framework for site-specific analysis and O&M policy selection of LEE damage for wind turbine blades. This approach can serve to study different maintenance strategies at the planning stage, anticipate the degradation rates of different coating solutions and plan inspections/maintenance at wind farm level. This framework is able to accommodate the uncertainty that lies in the coating behaviour and degradation dynamics, weather and maintenance success. The definition of a reliability function $g(x)$ allows for the quantification of the PoF of the chosen maintenance strategies. By selecting the appropriate cost metric and combining it with the probability of failure, a maintenance strategy can be chosen by adjusting the balance between cost and PoF to meet the policy of the organisation in charge of the operation of the asset. While suboptimal policies are achieved by not considering the actual condition and material properties of the component of the turbine being operated, this can serve as a baseline for the O&M of the asset while policies based on inspection/SHM are deployed. The adoption of predictive maintenance techniques can be a complicated and costly task if not performed in a structured approach and counter-producing if not executed properly. Therefore, improvements in the O&M shall be deployed in a staged way and with the aid of preanalysis based on models of the assets and the environment. The detailed knowledge of the dynamics of the most risk-critical failure modes requires an exhaustive analysis of all the uncertainties surrounding it. Once this knowledge is acquired, different failure modes can be analysed and combined through the use of surrogate models to provide computationally affordable representations of the asset that allow the study of combined failure modes, such as proposed in [28]. Given the potential catastrophic failures that a high-risk O&M policy can produce, numerical models emerge as a key tool to unveil further O&M cost reductions. Condition-based maintenance is more common for other components of the turbine such as the drivetrain, for which advanced data-based predictive models are developed, not without the difficulty of dealing with different parameters, logging frequencies and equipment manufacturers. In the case of the blade, it is not yet clear for the industry what failure modes to monitor, for which a risk analysis at component level is highly important [29].

Given the highly dimensional state space that this problem entails, condition-based maintenance design is not a trivial task. A promising strategy to extract insightful information is the use of Reinforcement Learning (RL) agents to try to discover and exploit interesting policies. While this technique requires a careful definition of the problem, reward function and parameters among others, the outcomes can be of great importance for the iteration towards optimal policies. A promising follow-up study would be the comparison of the proposed maintenance strategies with condition-based policies discovered through autonomous decision-making systems.

CRediT authorship contribution statement

Javier Contreras Lopez: Writing – review & editing, Writing – original draft, Visualization, Software, Methodology, Investigation, Formal analysis, Data curation, Conceptualization. **Athanasios Kolios:** Writing – review & editing, Supervision, Project administration, Funding acquisition, Conceptualization. **Lin Wang:** Writing – review & editing, Methodology, Conceptualization. **Manuel Chiachio:** Writing – review & editing, Methodology, Funding acquisition, Conceptualization. **Nikolay Dimitrov:** Writing – review & editing, Methodology, Conceptualization.

Declaration of competing interest

The authors declare that they have no known competing financial interests or personal relationships that could have appeared to influence the work reported in this paper.

Data availability

Data will be made available on request.

Acknowledgements

This study is part of the ENHAnCE project that has received funding from the European Union's Horizon 2020 research and innovation programme under the Marie Skłodowska-Curie grant agreement No 859957. Weather data was made available by the FINO (Forschungsplattformen in Nord-und Ostsee) initiative, which was funded by the German Federal Ministry of Economic Affairs and Energy (BMWi) on the basis of a decision by the German Bundestag, organised by the Projekttraeger Juelich (PTJ) and coordinated by the German Federal Maritime and Hydrographic Agency (BSH). CFD results were obtained using the ARCHIE-WeSt High Performance Computer (www.archie-west.ac.uk) based at the University of Strathclyde.

Appendix A. Repair success probabilities

See Tables A.6–A.8.

Appendix B. Acronyms

- **AEP**: Annual Energy Production
- **ANN**: Artificial Neural Network
- **BEM**: Blade Element Momentum
- **CFD**: Computational Fluid Dynamics
- **EoL**: End of Life
- **FSI**: Fluid-Structure Interaction
- **LEE**: Leading Edge Erosion
- **LEP**: Leading Edge Protection
- **MCS**: Monte Carlo Simulation

Table A.6
P_1 probabilities.

	0 (Inspection)	1	2	3	4	5	6
Jan	0.6614	0.6614	0.6614	0.6614	0.6614	0.3665	0.3665
Feb	0.7075	0.7075	0.7075	0.7075	0.7075	0.4052	0.4052
Mar	0.7194	0.7194	0.7194	0.7194	0.7194	0.4138	0.4138
Apr	0.8004	0.8004	0.8004	0.8004	0.8004	0.4807	0.4807
May	0.8138	0.8138	0.8138	0.8138	0.8138	0.4812	0.4812
Jun	0.8533	0.8533	0.8533	0.8533	0.8533	0.5326	0.5326
Jul	0.8663	0.8663	0.8663	0.8663	0.8663	0.5356	0.5356
Aug	0.8388	0.8388	0.8388	0.8388	0.8388	0.5083	0.5083
Sep	0.7908	0.7908	0.7908	0.7908	0.7908	0.4722	0.4722
Oct	0.7169	0.7169	0.7169	0.7169	0.7169	0.3162	0.3162
Nov	0.6880	0.6880	0.6880	0.6880	0.6880	0.3813	0.3813
Dec	0.6605	0.6605	0.6605	0.6605	0.6605	0.3841	0.3841

Table A.7
P_2 probabilities.

	0 (Inspection)	1	2	3	4	5	6
Jan	0.8444	0.7615	0.7243	0.6891	0.4624	0.1000	0.1000
Feb	0.8653	0.7925	0.7595	0.7281	0.5264	0.1000	0.1000
Mar	0.8832	0.8186	0.7892	0.7611	0.5715	0.1000	0.1000
Apr	0.9071	0.8544	0.8298	0.8062	0.6418	0.1000	0.1000
May	0.9070	0.8556	0.8317	0.8088	0.6483	0.1000	0.1000
Jun	0.9191	0.8728	0.8514	0.8307	0.6846	0.1000	0.1000
Jul	0.9221	0.8772	0.8514	0.8356	0.6921	0.1000	0.1000
Aug	0.8945	0.8369	0.8103	0.7849	0.6118	0.1000	0.1000
Sep	0.8912	0.8314	0.8037	0.7772	0.5964	0.1000	0.1000
Oct	0.8442	0.7597	0.7216	0.6856	0.4571	0.1000	0.1000
Nov	0.8303	0.7409	0.7006	0.6624	0.4264	0.1000	0.1000
Dec	0.8412	0.7576	0.7198	0.6840	0.4567	0.1000	0.1000

Table A.8
P_3 probabilities.

	0 (Inspection)	1	2	3	4	5	6
Jan	0.9614	0.9414	0.9309	0.9191	0.8066	0.1000	0.1000
Feb	0.9613	0.9409	0.9302	0.9196	0.8124	0.3930	0.3779
Mar	0.9680	0.9510	0.9417	0.9321	0.8387	0.1000	0.1000
Apr	0.9703	0.9538	0.9449	0.9352	0.8432	0.4560	0.4560
May	0.9708	0.9550	0.9463	0.9374	0.8502	0.4124	0.4124
Jun	0.9666	0.9481	0.9383	0.9281	0.8320	0.2432	0.2571
Jul	0.9751	0.9606	0.9383	0.9446	0.8645	0.3236	0.2991
Aug	0.9689	0.9521	0.9433	0.9342	0.8447	0.6747	0.6898
Sep	0.9703	0.9545	0.9459	0.9369	0.8510	0.2917	0.2917
Oct	0.9590	0.9353	0.9223	0.9095	0.7857	0.1000	0.1000
Nov	0.9630	0.9425	0.9316	0.9199	0.8057	0.1000	0.1000
Dec	0.9690	0.9534	0.9447	0.9359	0.8492	0.1000	0.1000

- **PoF**: Probability of Failure
- **RET**: Rain Erosion Tester
- **RL**: Reinforcement Learning
- **SPIFT**: Single Point Impact Fatigue Tester
- **WARER**: Whirling Arm Rain Erosion Test Rig

References

[1] Lozano-Minguez E, Kolios AJ, Brennan FP. Multi-criteria assessment of offshore wind turbine support structures. Renew Energy 2011;36(11):2831–7.

[2] Laura C-S, Vicente D-C. Life-cycle cost analysis of floating offshore wind farms. Renew Energy 2014;66:41–8.

[3] Maienza C, Avossa A, Ricciardelli F, Coiro D, Troise G, Georgakis CT. A life cycle cost model for floating offshore wind farms. Appl Energy 2020;266:114716.

[4] Scheu MN, Tremps L, Smolka U, Kolios A, Brennan F. A systematic failure mode effects and criticality analysis for offshore wind turbine systems towards integrated condition based maintenance strategies. Ocean Eng 2019;176:118–33.

[5] Nielsen JS, Sørensen JD. Methods for risk-based planning of O&M of wind turbines. Energies 2014;7(10):6645–64.

[6] Nielsen JJ, Sørensen JD. On risk-based operation and maintenance of offshore wind turbine components. Reliab Eng Syst Saf 2011;96(1):218–29.

[7] Morato PG, Papakonstantinou K, Andriotis C, Nielsen JS, Rigo P. Optimal inspection and maintenance planning for deteriorating structural components through dynamic Bayesian networks and Markov decision processes. Struct Saf 2022;94:102140.

[8] Nielsen JS, Tcherniak D, Ulriksen MD. A case study on risk-based maintenance of wind turbine blades with structural health monitoring. Struct Infrast Eng 2021;17(3):302–18.

[9] Nielsen JS, Sørensen JD, Sperstad IB, Welte TM. A Bayesian network based approach for integration of condition-based maintenance in strategic offshore wind farm o&m simulation models. In: Life-cycle analysis and assessment in civil engineering: towards an integrated vision. Taylor & Francis; 2018.

[10] Dimitrov N. Risk-based approach for rational categorization of damage observations from wind turbine blade inspections. J Phys: Conf Ser 2018;1037(4):042021.

[11] Bladena, Vattenfall, EON, Statkraft, Engie, x Thomsen K. INSTRUCTION: Blade inspections. Tech. rep., Bladena; 2016.

[12] Bladena, Vattenfall, EON, Statkraft, Engie, x Thomsen K. The blade handbook. Tech. rep., Bladena; 2021.

[13] Froese M. 3M to launch wind protection tape 2.0 at WindEnergy hamburg. Wind Power Eng 2016;9.

[14] Mischnaewski III L, Mishnaevsky Jr L. Structural repair of wind turbine blades: Computational model for the evaluation of the effect of adhesive properties. Wind Energy 2021;24(4):402–8.

[15] Mishnaevsky Jr L, Hasager CB, Bak C, Tilg A-M, Bech JI, Rad SD, et al. Leading edge erosion of wind turbine blades: Understanding, prevention and protection. Renew Energy 2021;169:953–69.

[16] López JC, Kolios A, Wang L, Chiachio M. A wind turbine blade leading edge rain erosion computational framework. Renew Energy 2023;203:131–41.

[17] Hersbach H, Bell B, Berrisford P, Hirahara S, Horányi A, Muñoz-Sabater J, et al. The ERA5 global reanalysis. Q J R Meteorol Soc 2020;146(730):1999–2049.

[18] Ravishankara AK, Özdemir H, van der Weide E. Analysis of leading edge erosion effects on turbulent flow over airfoils. Renew Energy 2021;172:765–79.

[19] Kruse EK. A method for quantifying wind turbine leading edge roughness and its influence on energy production. DTU Vindenergi; 2019.
[20] Johansen N. Test methods for evaluating rain erosion performance of wind turbine blade leading edge protection systems [Ph.D. thesis], Technical University of Denmark; 2020.
[21] Norris JR, Norris JR. Markov chains. no. 1, 2. Cambridge University Press; 1998.
[22] Forschungs- und Entwicklungszentrum Fachhochschule Kiel GmbH. Forschungsplattformen in Nordund Ostsee Nr. 1, 2, 3.. 2022, data retrieved from FINO1 Database, https://www.fino-offshore.de/de/index.html.
[23] Yi Y, Sørensen JD. Reduction of operation and maintenance cost for wind turbine blades–reliability model. Department of Civil Engineering, Aalborg University; 2019.
[24] Nielsen JS, Sørensen JD. Framework for risk-based optimal planning of O&M and inspections: Work Package 4–deliverable 4.5. Tech. rep, European Commission; 2017.
[25] Jonkman J, Butterfield S, Musial W, Scott G. Definition of a 5-MW reference wind turbine for offshore system development. Tech. rep, National Renewable Energy Lab.(NREL), Golden, CO (United States); 2009.
[26] Hasager CB, Vejen F, Skrzypiński WR, Tilg A-M. Rain erosion load and its effect on leading-edge lifetime and potential of erosion-safe mode at wind turbines in the north sea and baltic sea. Energies 2021;14(7):1959.
[27] Hasager C, Vejen F, Bech J, Skrzypiński W, Tilg A-M, Nielsen M. Assessment of the rain and wind climate with focus on wind turbine blade leading edge erosion rate and expected lifetime in Danish seas. Renew Energy 2020;149:91–102.
[28] Saleh A, Chiachío M, Salas JF, Kolios A. Self-adaptive optimized maintenance of offshore wind turbines by intelligent Petri nets. Reliab Eng Syst Saf 2023;231:109013.
[29] Lopez JC, Kolios A. Risk-based maintenance strategy selection for wind turbine composite blades. Energy Rep 2022;8:5541–61.